INNERVATION PATTERNS OF MYSTACIAL VIBRISSAE SUPPORT ACTIVE TOUCH BEHAVIORS IN CALIFORNIA SEA LIONS (*ZALOPHUS CALIFORNIANUS*)

A Thesis

by

CAITLIN DEMING SPROWLS

Submitted to the Office of Graduate and Professional Studies of
Texas A&M University
in partial fulfillment of the requirements of the degree of

MASTER OF SCIENCE

Chair of Committee,	Christopher D. Marshall
Committee Members,	Bernd Würsig
	Anja Schulze
Intercollegiate Faculty Chair,	Anna Armitage

December 2017

Major Subject: Marine Biology

ABSTRACT

Vibrissae, or whiskers, are highly developed sensory structures found in mammals. The follicles are referred to as Follicle Sinus Complexes (F-SC) due to the blood-filled sinuses. F-SCs are highly innervated compared to pelage. The most well-known group of vibrissae, mystacial vibrissae, are found around the muzzle in mammals. Pinnipeds have the largest and most innervated vibrissae of any mammal. More aquatic mammals tend to have larger F-SCs and greater innervation investment (axons per F-SC). Behavioral performance studies have shown that California sea lions *Zalophus californianus* (CSL, an otariid) excel at haptics whereas harbor seals *Phoca vitulina* (a phocid) excel at hydrodynamic trail following. The data presented in this thesis will infer vibrissal function from these studies. To date there has been no thorough investigation of innervation investment in an otariid. The objectives of this study were to investigate the innervation of the largest F-SCs, compare the innervation and microstructure to the most medial F-SCs, and compare the dorsal to ventral F-SCs. Follicles were dissected from tissues obtained from stranding programs and processed for histology. Axons were counted from wet mounted cross-sections. Asymmetry of axon bundles was present in all F-SC cross sections and have not been described before as well as blood vessels seen entering the DC of the LCS. There was a mean of 75±5 F-SCs per face muzzle. Innervation increased from medial (705 ±125 axons/F-SC) to lateral (1447±154) as well as from dorsal (541 ± 60) to the ventral F-SCs (1493 ± 327). Lateral F-SCs axon counts were similar to those in other pinniped studies. The total innervation from lateral axon

counts (108,525 axons) agree with other studies but total innervation from all six areas (86,042 axons) was 20% less than values from only lateral F-SCs. Axon density of medial F-SCs were significantly more than lateral F-SCs. This finding is congruent with CSL behavioral performance data that suggest they excel at haptic touch. We found no substantial evidence to differentiate which F-SCs fall into micro- or microvibrissae categories. To date no study has investigated the dorsal-ventral micro anatomical and innervation patterns in any pinniped.

CONTRIBUTORS AND FUNDING SOURCES

This work was supervised by a thesis committee consisting of Dr. Christopher Marshall, Anja Schulze of the Department of Marine Biology and Dr. Bernd Würsig of the Department of Wildlife and Fisheries.

The samples were collected and analyzed by the student, with the help of undergraduate volunteers Kelsey Johnson, Aubree Jones, Kenzie Merill, Dan Chaviers and Chris Givens.

This work was made possible in part by the Texas A&M University at Galveston Marine Biology Department. Its contents are solely the responsibility of the authors and do not necessarily represent the official views of the Marine Biology Department.

ACKNOWLEDGMENTS

I thank my advisor Dr. Christopher Marshall for his guidance and support. His never-ending informational support and financial assistance were extremely influential in completing my thesis. I will forever be grateful for your patience and time. Also, a sincere thanks to my committee members Anja Schulze and Bernd Würsig for helping me complete my thesis. And a huge thank you to my mom for keeping me reasonable and always believing in me, even when I wasn't sure I'd make it.

Thank you to the Marine Biology Department at A&M Galveston University for their financial support and their helpful staff members who always answer all of my questions. Lastly, sincerest of thanks to every single member of the Ecomorph lab the many lab interns that graciously volunteered their time to help me with my project, and the ones who were just there for moral support. The camaraderie, of this lab is like nothing I've ever seen before and it was so wonderful to be in such a supportive environment.

NOMENCLATURE

CSL……California sea lion

CT……...Collagenous Trabeculae

DC……...Dermal Capsule

DVN……...Deep Vibrissal Nerve

F-SC……...Follicle-Sinus Complex

GM……Glassy Membrane

HP.....Hair Papilla

HS……...Hair Shaft

ICB……Inner Conical Body

IRS.....Inner Root Sheath

LCS……Lower Cavernous Sinus

mm……Millimeters

MS……...Mesenchymal Sheath

NES……....Northern Elephant Seal

ORS……Outer Root Sheath

RS……...……Ring Sinus

RW……...Ringwulst

SA……...Surface Area

SD……...Standard Deviation

SG……Sebaceous Gland

UCS…….....Upper Cavernous Sinus

TABLE OF CONTENTS

LIST OF FIGURES

Page

LIST OF TABLES

Page

1. INTRODUCTION

Vibrissae, or whiskers, are highly developed sensory structures found in mammals. They are specialized hairs that differ from normal body hair. These structures consist of blood filled sinuses and several concentric layers of specialized tissues that surround the hair shaft and are highly innervated. Due to the blood sinus arrangement, they are more appropriately referred to as Follicle-Sinus Complexes (F-SCs). As in any hair, most structures reside within a follicle deep to the skin. The hair shaft grows from the base of the hair follicle (hair papilla) deep within the follicle and extends out of the follicle, through the follicular opening and into the environment. The majority of the hair shaft is exposed to the environment, and minute water movement or movement from active touching (haptic sense) are transmitted to the mechanoreceptors inside the F-SCs allowing the animal to detect changes in the environment. Vibrissae can be located all over the body in some mammals, but they are typically found in locations around the head (King 1991, Reep et al. 2002, Sarko et al., 2007, Drake et al 2015). The largest and best-known group is around the nose and muzzle consists of mystacial vibrissae. These structures have been well studied in terrestrial mammals such as rodents, cats, and even monkeys but have not been explored as thoroughly in aquatic mammals. Rodent F-SCs are typically innervated by 100-170 axons while cats possess approximately 215 axons per F-SC (Rice et al. 1986). Other aquatic mammals such as odontocetes possess vibrissae *in utero* but they degrade quickly before birth, or soon

after (Ling 1977). River dolphins are an exception with vibrissal crypts where vibrissae would be located and at least in one some species, these are used for electroreception rather than tactile sensation (Czech-Damal et al. 2012).

Pinnipeds (seals, sea lions, fur seals and walruses) and sirenians (manatees and dugongs) are remarkable in their use of vibrissae. Pinnipeds have the largest vibrissae of any mammalian group and in general their largest F-SCs are innervated by 1,600 axons per F-SC or more (Ling 1977, Hyvärinen et al. 1989, Marshall et al. 2006, Hyvärinen et al. 2009, McGovern et al. 2015). Sirenians use their mystacial vibrissae for both sensation but also to manipulate their food (Marshall et al., 1998, 2000, 2003; Reep et al., 1998). It is clear that pinnipeds heavily rely upon their whiskers for using tactile sensation during foraging and exploring their environment. This highly evolved sensory system is used for foraging even when other senses, such as sight, are not possible at night or in low visibility conditions (Hyvärinen et al. 1989, Dehnhardt et al. 1994 and 2001). The fact that blind seals are observed in the wild successfully foraging and raising offspring speaks to the specializations of pinniped vibrissae (Hyvärinen et al. 1989).

The size of the nerve bundle and the number of axons innervating whiskers are a good proxy for whisker sensitivity or any type of innervated sensory modality (e.g., George and Holiday 2013, McGovern et al. 2015). There appears to be a relationship between innervation investment (axons per F-SC) and aquatic nature of mammals. That is, the number of axons per F-SC increases as mammalian taxa become more aquatic. For example, Hyvärinen et al. (2009) demonstrated that the innervation investment of

terrestrial pole cats (*Mustela putorius*), semi-aquatic European otters (*Lutra lutra*), and ringed seals (*Phoca hispida*) show a progression of less innervation investment in terrestrial mammals to more innervation investment in those that have moved back to the water permanently. There are 10x more axons per F-SC in the mystacial vibrissae of pinnipeds than terrestrial pole cats. Even comparison of terrestrial pole cats and a semi-aquatic otter, which are both mustelids, demonstrates that there are 5x more axons per F-SC in semi-aquatic European otters than pole cats (Hyvärinen et al. 2009). To date, most research on whiskers has focused on the largest and most lateral whiskers in aquatic mammals. However, Mattson and Marshall (2016) report interesting differences in innervation investment and morphometrics between the macro- and micro-vibrissae; the number of axons per F-SC decreases from macrovibrissae towards the medial, micro-vibrissae.

The vibrissae of pinnipeds also differ in their microanatomy compared to terrestrial mammals. The first major difference is the number of blood sinuses. Terrestrial mammals only possess two sinuses, the ring sinus (RS) and the lower cavernous sinus (LCS), while pinnipeds possess three. This extra cavernous sinus (the upper cavernous sinus, UCS) above the RS is not innervated and is hypothesized to function as thermal protection and keep the deeper mechanoreceptors near body temperature (Mauck et al. 2000). This upper cavernous sinus is the largest sinus and can comprise up to 60% of the total F-SC length (Marshall et al. 2006, Hyvärinen et al. 2009). Another large difference in pinnipeds' F-SC structure is that the deep vibrissal nerve (DVN) penetrates the dermal capsule (DC) at the bottom of the follicle unlike

terrestrial taxa, whose DVN penetrates the DC on the side near the ring sinus (RS). As a result, the DVN nerve in pinnipeds must course apically to innervate mechanoreceptors in the LCS, the RS, RW and beyond to the inner conical body (ICB). Behaviorally, many terrestrial mammals, rodents in particular, rhythmically move their vibrissae in a "whisking" motion, where whiskers are moved quickly back and forth in a stereotypical behavior when exploring an object or their environment (Wineski 1985, Grant et al 2013). Pinnipeds do not "whisk" their vibrissae, but instead protract their vibrissae anteriorly and retract posteriorly to lie next to their head. During such protraction, the tips of the vibrissae form a three-dimensional arc and this motion can be complex. Such behavior is used for both active touch (haptic sense) or hydrodynamic trail following. Hydrodynamic trail following is a behavior in which some pinnipeds can track the fluid vortices shedding off fleeing fish. During active touch experiments seals and sea lions move their heads back and forth over the stimuli using their macrovibrissae to sense the size of an object and then use their micro vibrissae as a tactile fovea for object recognition (Kastelein and van Gaalen 1988, Dehnhardt and Kaminski 1995, Catania and Remple 2004, Glaser et al. 2011, Hanke et al. 2013, Mattson and Marshall 2016); individual whiskers are not moved independently. Walruses are the exception; they can manipulate their food using only, their mystacial vibrissae independently (Marshall et al. 1997). Walruses and bearded seals (*Erignathus barbatus*) are benthic foragers and have more mystacial vibrissae on a broader muzzle, compared to other non-benthic feeding pinnipeds (Ling 1977, Marshall et al. 2006).

The type of vibrissal hair shaft varies among seals. While pinnipeds possess a similar F-SC structure, there is disparity in the shape of hair shafts between phocids (true or earless seals) and otariids (sea lion and fur seals). With the exception of bearded and monk seals, all phocids possess beaded or bumpy hair shafts, and all otariids and walruses possess smooth hair shafts. The beaded profile has received much attention and appears to function to reduce drag and decrease the noise:signal of tactile cues when using their vibrissae during trail following (Glaser et al. 2011; see Hanke et al., 2013 for a review). These morphological differences could be an indicator of differences in sensory sensitivity or microstructure. It has been shown behaviorally during experiments that both harbor seals (*Phoca vitulina)* and California sea lions (*Zalophus californianus*) can sense dipole stimuli, sinusoidal movements of a sphere, while still or during hydrodynamic trail following (Dehnhardt et al. 1998 and 2001, Glaser et al. 2011). In other words, both groups have a haptic and hydrodynamic trail following capability. However, California sea lions had slightly higher sensitivity to the dipole stimuli, while at rest (reviewed by Hanke et al. 2013. In another type of experiment using hydrodynamic trail following, harbor seals had a higher percentage of success than California sea lions when they started after a long delay or there was a curve in the trajectory of the trail (Glaser et al. 2011). The difference in shape of the hair shafts could have an impact on why phocids are better at following hydrodynamic trails (Glaser et al. 2011, Ginter et al 2010). Both species also are able to detect differences in shapes and sizes of objects by using haptic touch, but otariids are better at detecting the shapes and sizes more so than phocids (Dehnhardt 1994, Dehnhardt and Ducker 1996, Grant

2013). Additionally, California sea lions demonstrate an increased discrimination capability at haptic touch tasks compared to phocids. It is possible that the micro-vibrissae of California sea lions possess a greater innervation investment per F-SC than phocids. Innervation investment data in the macro- and microvibrissae of phocids are available but at this time no data are available for any otariid.

The trophic ecology of California sea lions is among the best known for pinnipeds. They are coastal, shallow divers and ubiquitous in many parts of their range. As mentioned above, they have the capability to use mystacial vibrissae for hydrodynamic trail following but they excel at using active touch. California sea lions feed, opportunistically, on a variety of prey items (Antonelis and Fiscus 1980, Garcia-Rodriguez and Aurioles-Gamboa, 2004). Seasonally abundant schooling fish and squid are their main prey choice when available (Antonelis and Fiscus 1980, Garcia-Rodriguez and Aurioles-Gamboa, 2004). Some of the most common fish species consumed are Pacific cutlass (*Trichiurus lepturus*), Pacific sardine (*Sardinops caeruleus*), plainfin midshipman (*Porichthys spp.*), northern anchovy (*Engraulis mordax*), myctophids, and Pacific mackerel (*Scomber japonicas*), depending on what rookery the sea lions come from (Garcia-Rodriguez and Aurioles-Gamboa, 2004). They have been used as an example of a "typical" otariid, when looking at active touch and hydrodynamic trail following (Dehnhardt et al. 1994, Glaser et al. 2011). The behavioral data show that otariids and phocids both use their vibrissae extensively while navigating and foraging underwater (Hyvärinen, 1989; Dehnhardt, 1994). Although some microanatomical work has been conducted on CSLs (Stephens et al. 1973), there are no data regarding number

of vibrissae, and their innervation investment and pattern of innervation; nor do any data exist that distinguish differences between their macro- and microvibrissae. California sea lions do have a tripartite blood sinus system that is similar to that reported for other pinnipeds (Stephens et al., 1973). However, this work did not investigate innervation investment or go into great detail on F-SC microstructure. The types mechanoreceptors and some follicular structures were described and it is clearly apparent that they depend on this highly developed tactile system. Three types of mechanoreceptors (Merkel cells, lamellar corpuscle, and lancet shaped terminals) were recognized, as well as some with free nerve endings (Stephens et al. 1973). Although a pattern of innervation and investment appears to be developing for phocid pinnipeds, it is unknown if otariid pinnipeds follow this same pattern. Therefore, the overarching goal of this thesis was to conduct a systematic and comprehensive investigation of innervation investment, patterns of innervation and a morphometric analysis of the microanatomy of California sea lions so that their form and function can be directly compared with similar data for phocid pinnipeds.

1.1 Objectives

The objectives of this study are:

1) quantify the innervation investment of the largest California sea lion F-SCs and their morphometrics to test the hypothesis that California sea lions fit the innervation pattern investment established for phocids,

2) quantify the innervation investment of California sea lion macro- and microvibrissae (F-SCs), and their morphometrics, across the mediolateral muzzle to test the hypothesis that California sea lions fit into a similar mediolateral innervation investment pattern as reported for phocids.

3) quantify the innervation investment of California sea lion F-SCs, and their morphometrics, dorsoventrally across the muzzle to test the hypothesis that innervation investment decreases from the ventrum to the dorsum of the mystacial vibrissal array.

1.2 Expected Results

I hypothesize that the largest F-SCs of California sea lions, an otariid, will fit the overall phocid pattern of innervation investment (i.e., similar number of axons per F-SC). This would suggest that the largest California sea lion whiskers are just as sensitive as those of phocids. I also predict that innervation investment of F-SCs, and their morphometrics will fall into the same pattern recently published for harp seals (*Pagophilus groenlandicus*). Furthermore, I predict that similar pattern of innervation investment will be established for a series of F-SCs in the dorsal-ventral placement on the muzzle. Since California sea lions excel at active touch performance tests, I predict that ventrally located F-SCs will have a greater innervation investment and be larger than dorsally located F-SCs.

2. METHODS

Eight California sea lion muzzles were obtained during necropsies at the Marine Mammal Center (Sausalito, California) under NOAA salvage permit No. 358-1585. Each muzzle was preserved separately in 10% formalin. The mystacial vibrissa on each muzzle were quantified and mapped. The four largest F-SCs from each of the ventrolateral regions (n=8 per individual) were carefully dissected out of each muzzle. At the time of dissection, the length (from the skin level to the tip) and diameters (major and minor axes) of the hair shafts were measured, as well as the upper cavernous sinus width, lower cavernous sinus width and total follicular length with digital calipers in millimeters. Once measured, the hair shafts were cut off at the skin surface and the follicles were placed in individual vials of 10% formalin until processing. Hair shafts were collected and stored for future investigations.

F-SCs were removed starting at row B (Figure 1) at the most ventro-medial whisker, and then every other follicle was dissected to investigate the difference in morphology and innervation investment of the follicles. Three F-SCs were collected from the central vertical column on both sides of four muzzles: the most dorsal central, one in the middle of the muzzle, and the most ventral follicle. Three follicles from two muzzles each (n=6) were marked with a fiducial mark (a slit in the DC) and then processed with the objective of understanding follicular orientation *in situ.* Each vibrissa was categorized based its location on the muzzle. The whiskers from columns 7-9 rows A-C were classified as lateral. Lateral central F-SCS were classified from row B and

columns 5 and 6. Columns 3 and 4 from row B were classified as medial central and columns 1 and 2 were classified as ventro-dorsal. The central vibrissae were taken from column 5 row D and the dorsal central vibrissae were taken from columns 3 and 4 row F. These sections are color coordinated in Figure 2. A total of 143 F-SCs were removed (N=143). The follicles removed from the left side of the muzzles were cross sectioned and follicles removed from the right side were longitudinally sectioned. Thirty cross sectioned whiskers were chosen for morphometries, providing a representation of all locations on the muzzle.

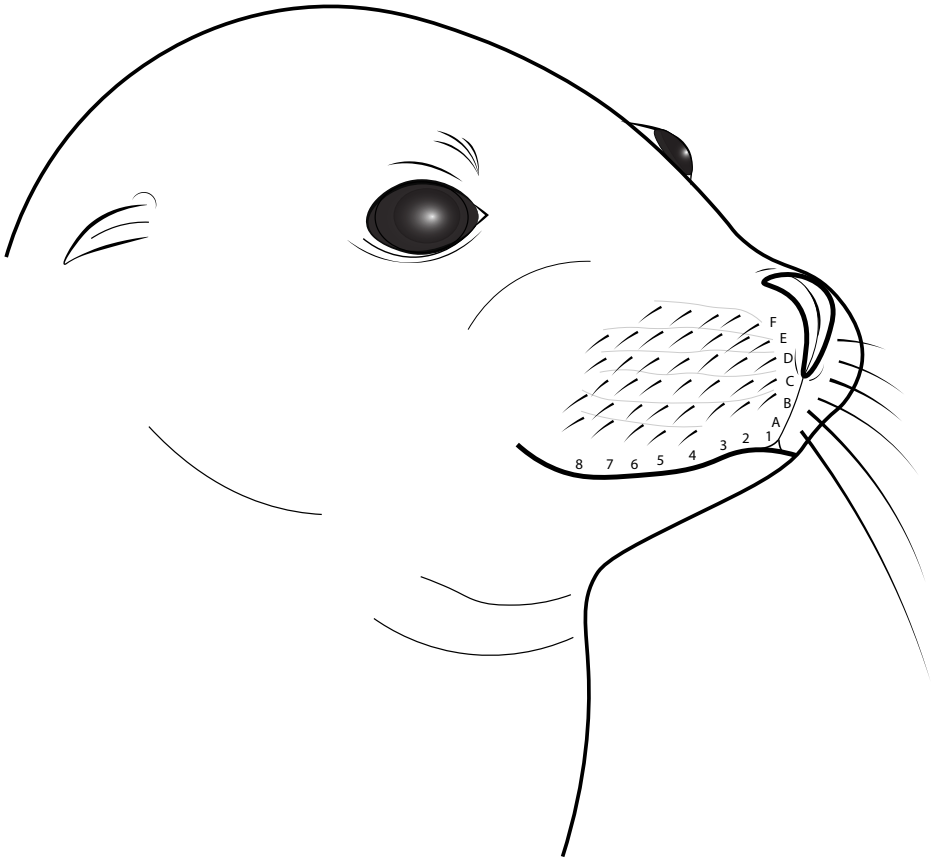

Figure 1. Map of California sea lions right side of muzzle. Showing organization of vibrissae in rows (A-F) and columns (1-8). *Whiskers not to scale to show location.

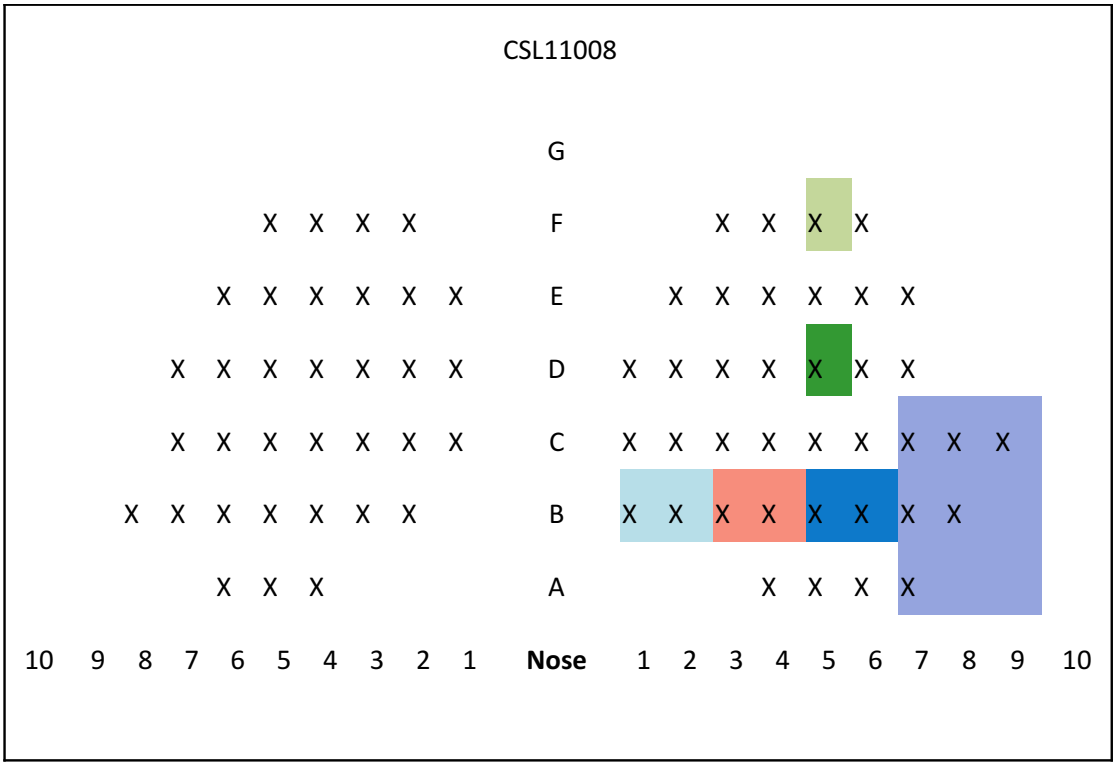

Figure 2. Representative map of face muzzle. CSL11008 specimens ID. Different vibrissal location categories are color coded. Light blue = ventro-medial, pink = medial central, dark blue = lateral central, purple = lateral, light green = dorsal central, dark green = central. Number indicate columns, Letters indicate rows. A total of 8 muzzles were mapped.

F-SCs were sectioned on a Lipshaw 80A freezing sliding stage microtome (Detroit, MI) at 25 µm. Since cross sections were used for axon counts, we focused on the LCS. Therefore, the UCS was removed and the follicle was sectioned from the RS to the lower margins of the LCS. Of the eight largest F-SCs collected (four per each side of all muzzles) four F-SCs were cross-sectioned and four were longitudinally sectioned for each animal. The longitudinal sections were stained using a modified Bodian silver, or a Masson's trichrome stain, or for axon counts not stained at all.

Longitudinal sections were mounted onto 1% glucose gel coated glass slides in series. The cross-sections were analyzed as wet mounts at 4X on a Nikon Eclipse E400 light microscope. Five of the best sections were selected from the middle of the LCS. Micrographs were taken at 40x using a Diagnostic Instruments (Sterling Heights, MI) microscopy camera and Spot Image Analysis software (Sterling Heights, MI) to quantify axon bundles and individual axons. All axons were counted from wet mounted sections. Axons were quantified at this location (lower cavernous sinus) since the deep vibrissal nerve doesn't start branching yet and counts at this location were representative of the true number of axons present (Reep et al., 1998). Collection of axon counts at this location is also consistent with other studies and therefore the data are comparable across species (Marshall et al. 2006, 2014, McGovern et al. 2015, Matson and Marshall, 2016). The individual axons in the bundles were quantified and marked as read using Adobe Photoshop and a manual clicker. Mean innervation of each F-SC was quantified by averaging all the axons in each cross-section across all five LCS sections per F-SC.

Follicle-Sinus Complex morphometric data were collected using SPOT software and the mean and SD of the three replications of each measurement was calculated. The longitudinal section morphometrics collected were: F-SC length, total sinus length, maximum ring sinus (RS) width, maximum dermal capsule (DC) thickness, maximum hair shaft (HS) diameter at the RS. Cross sectioned morphometrics were: maximum diameter of section including DC, maximum major and minor axis diameter of HS, DC at the thickest and thinnest points, collagenous trabeculae (CT) thickest and thinnest

points, and the mesenchymal sheath (MS) thickest and thinnest points, following Marshall et al. (2006, 2014), and Matson and Marshall (2016).

To investigate innervation investment independent of size, axon densities for each category were calculated (mean axon/surface area). The surface area, excluding the DC and HS areas, was measured from cross sections and then used to divide with the mean axon number to determine if there was difference in density based on location. Significant differences among densities in the different groups of follicles were tested using ANOVA and Tukey test in R (Hothorn et al. 2008).

3. RESULTS

3.1 Mystacial Vibrissal Array

The entire mystacial vibrissal array had a mean of 38±2 whiskers per side of the muzzle and 75±5 vibrissae per muzzle. The vibrissal array dimensions had a mean of 61.7 ± 11.914 mm wide and 49.0 ±6.319 mm long; the mean estimated surface area was 302.3 cm^2. Mystacial vibrissae were arranged in 6-7 rows and 7-9 columns. Overall, the length of each hair shaft increased medial-to-lateral as well as dorsal-to-ventral, with the longest hair shaft in the ventrolateral region. All hair shafts had a smooth structure; there were no beaded morphologies as reported for phocids. Table 1 summarizes the hair shaft lengths from each group of vibrissae and Figures 1 & 2 map the location of all mystacial whiskers and identify the groups sampled for histology from the mystacial vibrissal array.

Morphometrics were collected from the hair shafts during the mystacial vibrissal count and subsequent dissection of follicles from each muzzle as well as after histological processing. The mean lateral follicle length from dissected follicles was 13.03±1.21 mm. The maximum total follicle length was 15.3 mm and was collected from the lateral-most vibrissa; the smallest total follicle length was 3.15 mm located from the dorso-central vibrissa in the study. Mean follicle lengths for medial central and ventro-dorsal vibrissal follicle groups were similar at 4.69±0.644 and 4.08±0.428 mm, respectively. The follicular length in every other group was transitional among these

means. That is, follicular length increased dorso-central-ventrally and medio-central-laterally (Table 2).

Table 1. Summary of hair shaft lengths of each vibrissal location by category.

Vibrissal Category	Mean (mm)	S.D.	Length Range (mm)	HS Diameter 1(mm)	HS Diameter 2 (mm)	n=
Ventro-Medial	16.35	6.46	4.94 – 24.54	0.27	0.218	15
Medial Central	34.14	8.78	15.46 – 46.98	0.77	0.53	17
Lateral Central	66.58	25.04	11.25 – 101.11	1.27	0.94	25
Lateral	64.37	52.28	10.45 – 175	1.31	1.25	48
Dorsal Central	10.45	4.87	3.5 – 16.83	0.26	0.22	11
Central	50.26	8.44	37.38 – 62.64	0.98	0.811	10

Table 2. Summary of follicular length.

Vibrissal Category	Mean (mm)	S.D.	Min (mm)	Max (mm)	n=
Ventro-Medial	4.69	0.644	3.89	5.78	14
Medial Central	7.44	1.131	5.59	9.73	16
Lateral Central	11.33	1.419	8.45	14.61	25
Lateral	13.03	1.216	10.62	15.3	48
Dorsal Central	4.08	0.428	3.15	4.59	11
Central	8.72	0.68	7.65	8.72	10

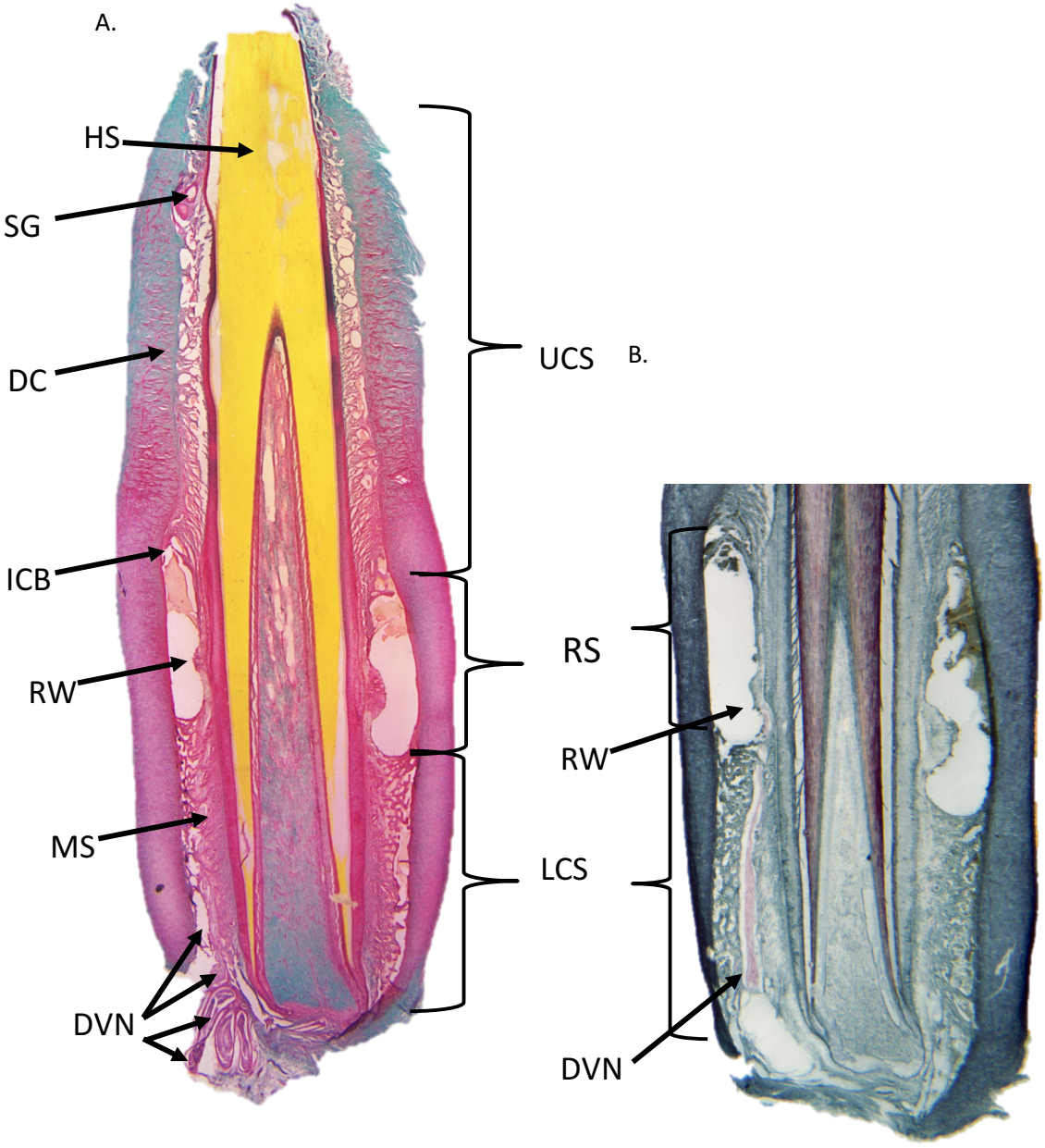

Figure 3. Longitudinal sections of F-SC through the middle of a lateral vibrissa. A. Center section of a F-SC stained with modified Trichrome. B. Section stained with modified Bodian Silver stain. DVN clearly seen as light red color running through LCS. LCS: lower cavernous sinus, RS: ring sinus, UCS: upper cavernous sinus, DVN: deep vibrissal nerve, MS: mesenchymal sheath, RW: ringwulst, ICB: inner conical body, DC: dermal capsule, and SG: sebaceous gland.

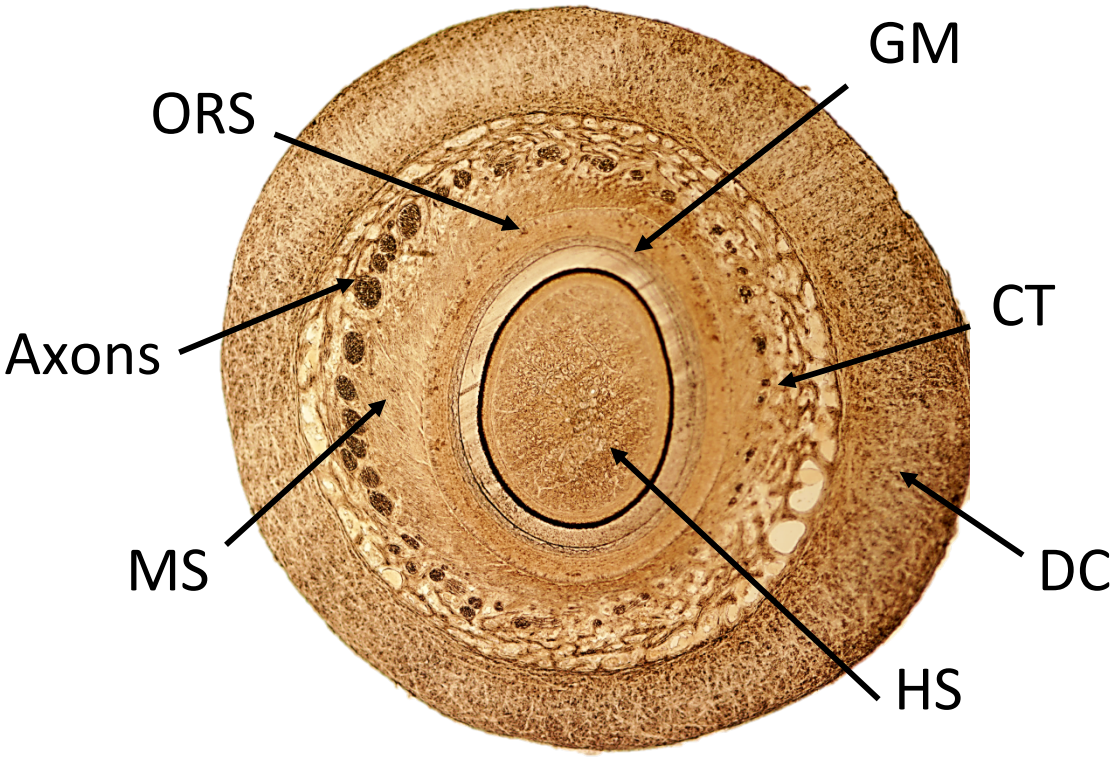

Figure 4. Cross-section through the middle of the LCS. Unstained axon bundles from a wet-mount section.

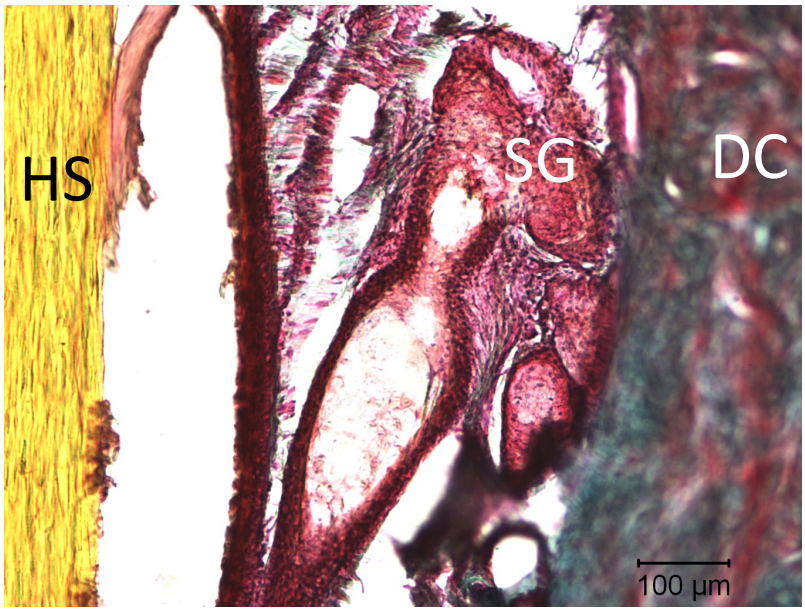

Figure 5. Sebaceous gland located in apical portions of the UCS. Note the duct leading from the gland to the hair-shaft.

3.2 F-SC Morphology

The microstructure and innervation patterns were similar in all follicles investigated. The overall structure of a vibrissa was comprised of a tripartite sinus (UCS, RS, and LCS; depicted in Figure 3). The glassy membrane (GM) was present throughout the LCS. The MS and CT were present in both the LCS and UCS, but not in the RS. The DC was the most superficial ring that surrounded the CT on the outside of the follicle (Figure 4). Axons were only found in CT. The MS was deep to the CT, between the CT and the GM, which surrounded the hair shaft of the follicle. The outer root sheath is located between the GM and IRS, which is next to the HS.

Typically, a single sebaceous gland (SG) was present in the apical portion of the UCS in each follicle (Figure 5). No other glands were observed. In addition to red blood cells commonly observed in each sinus, the UCS also exhibited vascularization in addition to blood cells. That is, actual vessels were apparent within the UCS. In some follicles, vessels could be observed penetrating the DC in the LCS (Figure 6). As in phocids, the DVN penetrated the F-SC at the base and coursed to the RS and inner conical body. Branches could be seen innervating presumed mechanoreceptors beginning at the mid to upper reaches of the LCS, into the RS and RW and the ICB. No innervation was observed in the UCS. In cross-sections, a marked asymmetry of the axon bundles was observed in all follicles throughout the LCS. All of the follicles with fiducial marks were from ventro-medial, medial central, and lateral categories (row B and from columns 2, 4, and 6, Figure 7). The thicker DC is always located laterally,

whereas the thinner part of the DC is medial. This asymmetry was present in all follicles (i.e., medial-lateral and dorsal-ventral).

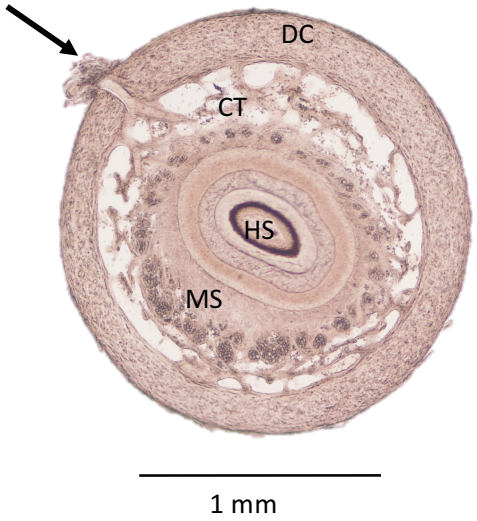

Figure 6. Arrow pointing to blood vessel entering DC within the LCS.

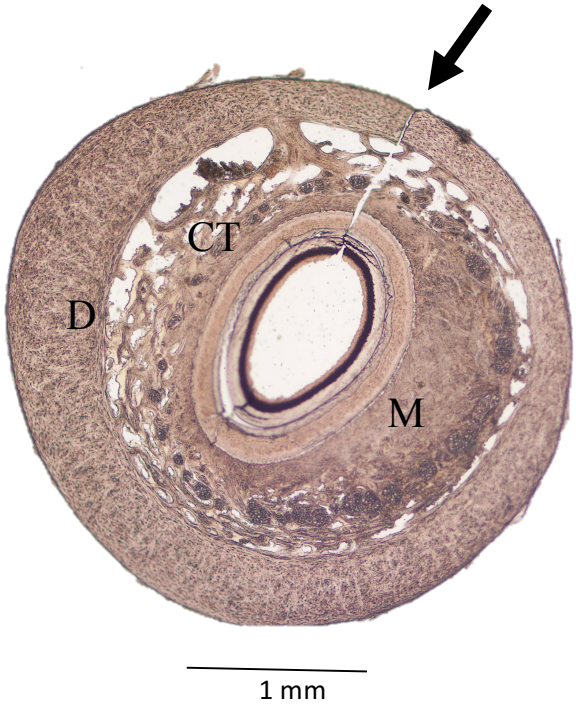

Figure 7. Fiduciary mark on cross-section of a lateral F-SC. Note that the HS missing from this section.

3.3 F-SC Morphometrics

Morphometric data of F-SCs are summarized in Table 3 & 4. The maximum diameter of a F-SC was 4.39 mm, which was observed in the lateral most follicle. The smallest diameter of 1.42 mm was observed in most medial follicle. Overall, as with the gross anatomical morphometrics, the histological follicular diameter increased from medial-to-lateral, as well as dorsal-to-ventral. The hair shaft ratio, ratio of major vs. minor hair shaft lengths in cross-section were similar (.65-.83) from all categories (Table 4) despite the differences in follicular diameter. The UCS comprised a mean 51% (±3.182% SD) of the total follicular length in the lateral vibrissae, 42% (±3.45% SD) in both the ventro-medial and central dorsal vibrissae, and 48% (±2.80% SD) in the central, medial central and lateral central vibrissae. The RS comprised 19% of total follicular length in the lateral F-SCs, 30% in ventro-medial F-SCs, 27% in the central dorsal F-SCs, and 22% in the medial central and lateral central F-SCs, respectively The LCS comprised approximately 30% for lateral central, dorsal central, and lateral follicles, and 28% for ventro-medial and medial central. The asymmetry of nerve bundle distribution is typically adjacent to the thickest section of the DC (Figures 4 and 8).

Table 3. Longitudinal morphometrics from each F-SC category in mm.

	Ventro-Medial	Medial Central	Lateral Central	Lateral	Dorsal Central	Central
Total F-SC length	4.87±1.55	10.93±2.58	12.03±0.823	11.77±0.617	4.24±0.871	8.35±1.12
Max DC width	0.31±0.107	0.71±0.068	0.66±0.106	0.75±0.014	0.31±0.047	0.57±0.041
Max RS width	0.43±0.187	0.44±0.149	0.52±0.067	0.55±0.074	0.37±0.064	0.44±0.038
% UCS	42.28±4.86	48.06±1.84	48.15±3.758	50.9±3.182	42.46±2.04	47.64±4.05
% LCS	28.13±7.21	28.61±2.31	30.84±4.24	29.87±1.99	30.4±0.545	27.44±2.25
% RS	29.59±2.81	23.33±0.883	21.01±3.23	19.22±1.20	27.14±1.49	24.93±1.81

Table 4. Cross-sectional morphometrics from each F-SC category in mm.

	Ventro-Medial	Medial Central	Lateral Central	Lateral	Dorsal	Central
Max diameter	1.64±0.213	2.64±0.185	3.59±0.213	3.85±0.318	1.73±0.094	3.13±0.159
Hair shaft ratio	0.73±0.068	0.65±0.049	0.75±0.053	0.78±0.036	0.84±0.066	0.78±0.015
DC thickest	0.22±0.043	0.45±0.048	0.63±0.056	0.74±0.114	0.23±0.025	0.57±0.079
DC thinnest	0.11±0.034	0.20±0.03	0.32±0.050	0.36±0.064	0.15±0.017	0.26±0.023
DC ratio	0.52±0.076	0.45±0.053	0.50±0.090	0.63±0.481	0.67±0.078	0.47±0.079
MS thickest	0.20±0.033	0.36±0.061	0.32±0.080	0.36±0.105	0.17±0.034	0.28±0.039
MS thinnest	0.04±0.030	0.07±0.020	0.09±0.039	0.12±0.032	0.05±0.013	0.09±0.012
CT thickest	0.29±0.057	0.36±0.047	0.49±0.062	0.45±0.083	0.32±0.046	0.40±0.051
CT thinnest	0.14±0.064	0.18±0.051	0.25±0.070	0.25±0.049	0.19±0.029	0.23±0.038

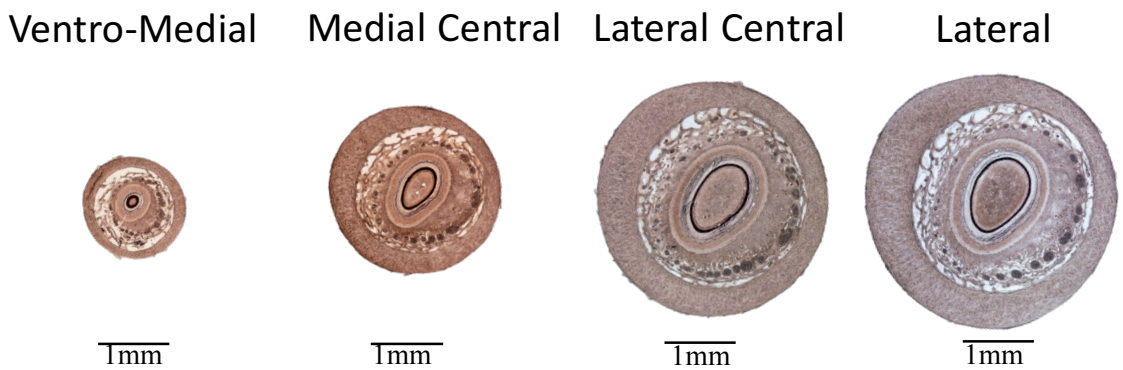

Figure 8. Medial-to-lateral cross-sections. Sections to scale and orientation depicting the decrease in diameter of vibrissal follicles

3.4 F-SC Innervation

The innervation investment (i.e., number of axons) increased medially to laterally. The mean axon count for the lateral category whiskers was 1447±154. The largest lateral axon count 1777 located in column 7, while the largest medial axon count was 802 located in column 2. The ventro-medial, medial central, and lateral central regions had a mean of 705 ±125, 1094 ± 204, and 1493 ± 327, respectively. There was also an increase in innervation investment from dorsal to ventral (Figures 9 and 10). The dorsal central mean axon count was 541 ± 60, the central mean axon count was 1095 ± 206. There were no clear distinctions between micro and microvibrissae based on axon count alone.

Axon density was significantly different ($p \leq 0.05$) among the ventro-medial and lateral, medial central, lateral central vibrissal categories (Figure 8). There was also a significant difference between the medial central and lateral vibrissae. There was not a significant difference in density among the dorsal central, central, medial central, and lateral central categories (Figure 11).

Total estimated innervation was calculated by multiplying the mean lateral-most axon count by the mean number of F-SC totaling about 108,525 axons. The corrected total innervation (the 10% decrease described by Mattson & Marshall 2016) was 97,673 axons. Due to the expanded investigation of innervation investment across the entire vibrissal array a new calculation was needed. Each of the six sections were taken into

consideration and multiplied by the amount of F-SCs in each section on the muzzle to create a total innervation.

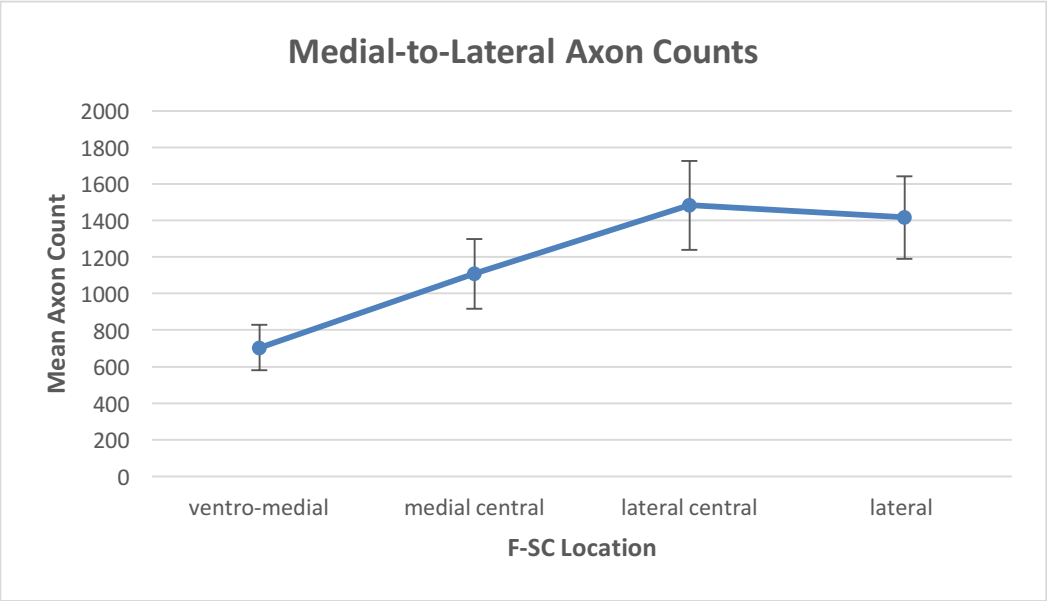

Figure 9. Mean axon counts with SD for medial-to-lateral.

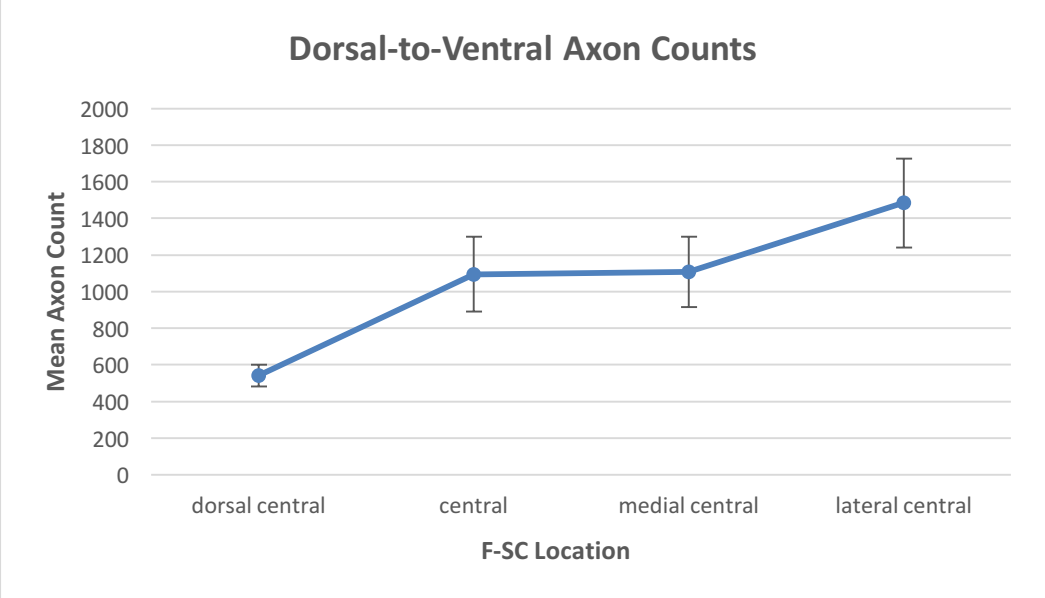

Figure 10. Mean axon counts with SD for dorsal-to-ventral

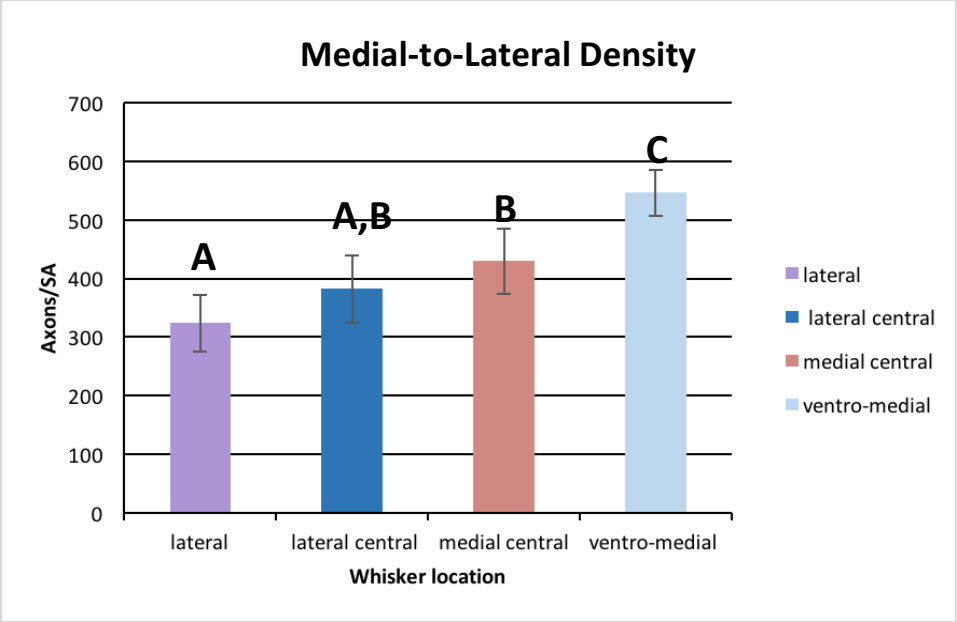

Figure 11. Density (Axons/SA) plots with SD showing significant differences from medial-to-lateral.

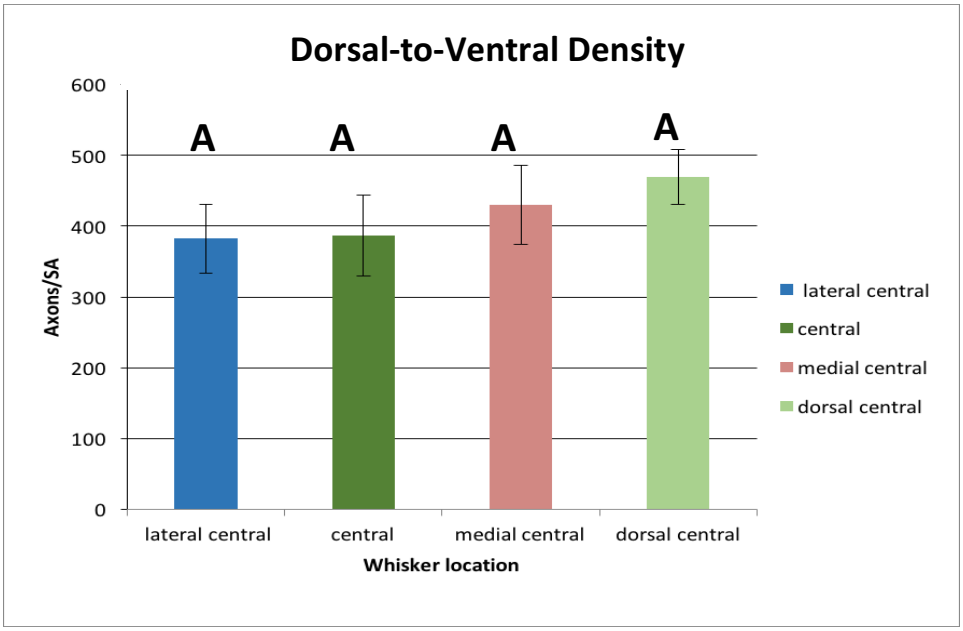

Figure 12. Density (Axons/SA) plots with SD showing no significant differences from dorsal-to-ventral.

4. DISCUSSION

4.1 Mystacial Vibrissal Array

Relative to those other pinnipeds, the total number of vibrissae in CSLs were similar with the exception of Ross *(Ommatophoca rossii)* and bearded seals (Ling 1972, Marshall et al. 2006). The longest hair shafts of CSLs (101 mm) in this study were similar to that reported for harp seals (106 mm, Mattson and Marshall 2016), harbor seals (100 mm, Jones 2017), ringed seals (*Phoca hispida,* 110 mm, Hyvärinen et al. 2009) but shorter than northern elephant seals (*Mirounga angustirostris*, 138 mm, McGovern et al. 2015). Our shortest F-SC length (1.95 mm) was shorter than other pinnipeds, but only one other study has investigated microvibrissae, where the shortest lengths would be located (Mattson and Marshall 2016). The maximum length is similar to what was reported in harp seals but the minimum was shorter than harp seals (12.2 mm) (Mattson and Marshall 2016). Therefore, CSL have a greater range of vibrissal hair shaft lengths compared to phocids for which data are available. However, these are estimates, as some hair shafts can be worn and broken over time. The age and sex of the specimens are unknown but should not affect the number of vibrissae on the muzzle, as mammals are born with a fixed number of follicles. The surface area of the CSL array were larger than harp seal vibrissal array (Mattson and Marshall 2016). There was no beaded morphology on the hair shafts as expected, since this feature has only been observed in phocids.

4.2 F-SC Morphology

California sea lions exhibited the same basic tripartite F-SC morphology reported for phocids and sea otters, with all the same concentric layers of tissue and a DVN entering the follicle at its base (Stephens et al. 1973, Marshall et al. 2014, McGovern et al. 2015, Mattson and Marshall 2016, Jones 2017). Observations regarding the microanatomy of the F-SC agrees with Stephens et al. (1973). Stephens et al. (1973), also reported blood vessels and the DVN entering the F-SC at the base together but this study differs in that separate blood vessels were observed entering through the DC of the LCS for the first time. Although vascularization was observed within the UCS, no blood vessels penetrating the DC in the UCS were observed as reported in northern elephant seals (McGovern et al. 2015). It is likely that blood vessels do penetrate the DC of the UCS in CSLs but these were not observed in this study. One sebaceous gland was found in the apical part of the UCS unlike sea otters (*Enhydra lutris*) and NES which exhibited multiple larger sebaceous glands located in this region (Marshall et al. 2014, McGovern et al. 2015).

California sea lions differed in the degree of asymmetry of the axon bundles within their F-SCs. CSLs axon distribution with in the CT showed asymmetry throughout their distribution across the muzzle, while harp seal axon bundles became more asymmetrical medial-to-lateral (Mattson and Marshall 2016). However, in CSL the more lateral follicles were less circular in circumference and the thickest part of DC tended to protrude to create a slight tear shape. The ratio of thickest to thinnest DC

showed no differences between medial and lateral follicles. Based on the orientation of F-SCs, verified with fiduciary marks, we hypothesize that the thickest DC on the lateral side of F-SC in the lateral-most follicles is due to muscle attachment as suggested by Mattson and Marshall (2016). Muscle attachment in these lateral F-SC need a greater range lateral of motion compared to more medial vibrissae. This suggests that CSLs use the lateral vibrissae differently than medial whiskers and this feature may be the most useful in constituting a functional division into micro- vs. macrovibrissae. There were no major differences between HS ratios, DC ratios, or asymmetry as seen by Mattson and Marshall 2016.

California sea lions, like most otariids, have a dolichocephalic head and snout compared to phocids and this results in a different placement and orientation of their mystacial vibrissae on the muzzle from those of phocids. These differences potentially change how they use their vibrissae (King 1991). Potential functional consequences could be an increase in the range of motion and the extent of vibrissal protrusion (forward movement of whiskers), which might explain why all the F-SCs are asymmetrical, not just lateral F-SCs as observed in harp seals (Mattson and Marshall 2016). Difference in rostral shapes is an underappreciated aspect of pinniped whisker function and performance.

4.3 F-SC Morphometrics

The hair shaft ratios (minor axis: major axis) were consistent throughout each of the regions sampled (ventro-medial, medial central, lateral central, lateral, central, and central dorsal). This differs from harp seals in which hair shafts were rounder (ratio closer to 1:1) and became more elliptical laterally (Mattson and Marshall 2016) (Table 5). The HS ratios of CSL are more similar to the HS ratios of medial F-SCs (columns 9-11) of harp seals (Mattson and Marshall 2016). CSL hair shafts are still elliptical but rounder than the lateral harp seal hair shafts (Table 5). There have been inconsistencies in the literature as to how the ratio of major and minor axes has been reported. Here we promote a scale of 0-1 with 1 being a perfect circle. For comparison, we have converted harp seal medial to lateral HS ratios and summarized them in Table 5. Table 6 shows the comparison of HS ratios in lateral F-SCs. The lateral HS ratio of CLSs is similar to all phocids in Table 6.

Table 5. Comparing CSL vs harp seals HS ratio formulas. Adapted from Mattson and Marshall 2016.

	Medial	Medial Central	Lateral Central	Lateral
CSL >1 ratio	1.37	1.56	1.34	1.28
Harp seals >1	1.24	1.56	1.83	1.95
CSL <1 ratio	0.73	0.65	0.75	0.78
Harp seals <1	0.78	0.65	0.61	0.60

Table 6. Comparative lateral HS ratios across pinnipeds. Adapted from Marshall et al. 2006, McGovern et al. 2015, and Mattson and Marshall 2016.

Species	Lateral HS ratio
CSL	0.78
Harp seal	0.60
NES	0.74
Bearded seal	0.60

The UCS ventro-medial and dorsal-central CSL follicles differed compared to other species reported since their proportion of total follicle length was < 50% (Hyvärinen 1989, Marshall et al. 2006, McGovern et al. 2015, Mattson and Marshall 2016, Jones 2017). The increase in UCS proportion is in more medial and dorsally located F-SCs suggesting a transition from micro- to macrovibrissae, but this is not as clear as reported in harp seals (Mattson and Marshall, 2016). The large proportion of the UCS has been hypothesized to function to thermally protect mechanoreceptors within the inner conical, RS and LCS (Mauck et al. 2000). Thermal images demonstrate that the individual follicles had much higher temperature than the surrounding tissue. Unlike ringed and bearded seals, CSL do not inhabit cold water habitats. Additionally, CSL are not deep divers (averaging 80 m under 3 min) as are elephant seals, which can dive for greater than 20 min at over 350 m depth, or ringed seals which usually dive less than 100 m for 10 to 15 min (Feldkamp et al. 1989, DeLong and Stewart 1991, Gjertz 2000). Those phocids that live in cold water habitats (e.g., ice seals) would require a larger UCS to thermally protect underlying mechanoreceptors, which are not necessary in CSL because

they are not like deep diving phocids (Rice et al. 1986, Dehnhardt et al. 1999, Mauck et al. 2000, Hyvärinen et al. 2009). In addition to the decrease in the proportion of the UCS, the proportion of the RS also decreased in more ventral and laterally located F-SCs. Comparatively, the RS proportion in ventrolateral F-SC is in the same range as other phocids (Ling 1966, Marshall et al. 2006, McGovern et al. 2015, Mattson and Marshall 2016, Jones 2017). It is worth noting that the smaller follicles that have a proportionally reduced UCS would necessarily have a proportionally greater RS. An increased RS proportion could be inferred to increased number or density of mechanoreceptors (which is outside the scope of this study). The proportion of the LCS was similar across all F-SCs for CSL, and similar to phocids. The LCS proportion was ~30 – 40% of the total follicular length (Ling 1966, Marshall et al. 2006, McGovern et al. 2015, Mattson and Marshall 2016, Jones 2017).

4.4 F-SC Innervation

Most work regarding phocid vibrissae has only investigated lateral mystacial vibrissae. Therefore, it is impossible to conduct a broad comparison as no one has looked at both medial-to-lateral and dorsal-to-ventral vibrissae. The axon counts from CSL lateral vibrissae are in the same range of axon counts as other phocids studied (Marshall et al. 2006, Hyvärinen et al. 2009, McGovern et al. 2015, Mattson and Marshall et al. 2016, Jones 2017). The only other study that has looked at the transition from medial to lateral was Mattson and Marshall (2016) in harp seals. The mean axon count for ventro-medial F-SCs was higher in CSL (705 ±125) vs. harp seals (555 ± 97.4; Mattson and Marshall 2016).

To date no study has investigated the dorsal-ventral microanatomical and innervation patterns in any pinniped. Past studies assumed a similar level of innervation in the lateral F-SC throughout the mystacial vibrissal array, and this was used to estimate total F-SC investment (Marshall et al. 2006). However, such assumptions underestimate total innervation by ~10% (Mattson and Marshall 2016). However, since much of the comparative data estimates total innervation based on the largest, lateral F-SCs it is still a useful measure. Based on only the largest, lateral F-SCs, CLS are estimated to have a total innervation of 106,275 axons/muzzle. Correcting that estimate by 10% provides a total of 96,670 axons. In this study, we took into account all six of the regional mystacial areas by calculating the mean axon count for each area and multiplying that by the number of whiskers in that area. Using this estimate the total innervation should be

86,042 axons, which is ~20% lower than the estimated total using just lateral vibrissae. However, additional similar work should be conducted on phocids to assure that this is a pinniped pattern and not an otariid or phocid pattern. In terms of innervation there does not seem to be a clear distinction between macro- and microvibrissae in CSLs. There is no distinct inflection point in number of axons between medial and lateral F-SCs as reported for harp seals (Mattson and Marshall 2016). When observed CSL used their first three columns of vibrissae to target the object. This is where our best guess would be in terms of dividing macro and microvibrissae. There are other aspects that could be involved that can define micro and macrovibrissae that are not morphological and were not looked at in this study. Continued studies into CSL F-SC innervation may find new mechanoreceptors as found in Florida manatees (*Trichechus manatus latirostris*), in which the medial F-SCs differed from the lateral (Sarko et al., 2007). Such differences would have strong functional inference that could more clearly delineate macro vs microvibrissae.

The axon density was another way to compare innervation investment to other pinnipeds (i.e. harp seals) and other areas on the muzzle. There were significant differences medial to lateral in axon density. However, there was no significant difference between dorsal and ventral F-SCs in regards to axon density (Figures 9 & 10). There is an increased density in dorsally located F-SCs indicating a trend similar to medial to lateral, and with increased sample size there could be a significant difference (Figure 10). The medial density was greatest (550) which agrees with the haptic touch behavioral performance work of CSL (Dehnhardt 1994, Dehnhardt et al. 1996). The

density of harp seal medial F-SCs (490 axons/SA) F-SCs were greater than in the lateral (297.7 axons/SA) follicles but there was not as great of a difference between medial and lateral compared to CSL.

4.5 Comparison

California sea lion mystacial vibrissae differ enough in their distribution, microanatomy, morphometrics and innervation to warrant their own designated otariid pattern. They possess greater innervation within their medial micro-vibrissae compared to harp seals, and this level of innervation is similar to their dorsal F-SCs. Their distribution of micro- vs. macrovibrissae is not as distinguishable as observed in harp seals (Mattson and Marshall 2016). Their vibrissal microanatomy differs in that the HS ratio is the same throughout the muzzle, there is vascularization in the UCS, and penetrating blood vessels into the LCS which have not been documented previously. The proportion of the UCS to follicular length decreases in more medial and dorsally located F-SC, which was not observed in harp seals (Mattson and Marshall 2016).

The innervation and microstructural patterns observed in CSLs, which for the time being could be considered an otariid pattern, does not show distinct differences between micro-and macrovibrissal fields, but is instead more of a gradual change in terms of innervation and microstructure. The morphometric data presented here, and from personal observations of actual mystacial whisker function in live CLSs, the first four medial columns function for object recognition during active touch behaviors and should be considered as microvibrissae. Although CSLs vibrissal tactile performance

data using active touch indicates that a tactile fovea incorporates microvibrissal use, and macrovibrissae for object recognition and orientation (Dehnhardt 1994, Dehnhardt et al. 1996), the morphological distinctions are less clear than the behavioral distinctions. More detailed studies focusing on mechanoreceptor diversity and density between lateral and medial vibrissae are likely to yield important functional mechanisms that support for these behavioral observations. Unlike terrestrial mammalian vibrissal studies, which have measured vibrissal row, HS length, and distribution of vibrissae to distinguish micro- and macrovibrissae (e.g., Brecht et al. 1997), the distribution of CSL mystacial vibrissae has clear rows but no distinct clustering of microvibrissae, nor do they exhibit the distinct morphological change in symmetry as observed in harp seals (Mattson and Marshall, 2016). Since this is the first otariid whose mystacial vibrissae have been investigated at this detailed level, studies of additional otariid species are needed to confirm if patterns observed in CSL are typical of all otariids or not. Furthermore, it would be beneficial to investigate other mystacial vibrissal areas (i.e., microvibrissae) in phocids already examined to obtain a more complete data set.

The evolution of hair is still an imprecise area of study since hair does not fossilize. However, it is known that the first hairs were vibrissal-like (Chernova 2006), and while vibrissae do not appear in the fossil record, observation of extant aquatic mammals suggests that strong selection pressures greatly changed their innervation and function. Since pinnipeds transitioned back to aquatic habitats approximately twenty-seven million years ago their tactile sensory system adapted quickly (Berta 2009). Pinnipeds and sea otters possess a highly-refined sense of touch that is much more

sensitive than semi-aquatic and terrestrial mammals (Hyvärinen et al. 2009). Among this group, terrestrial mammals have the least number of axons per F-SC. Semi-aquatic animals, such as Australian water rats (*Hydromys chrysogaster*) and the European river otter tend to show an increase in their innervation (363 and 350 axons/F-SC, respectively) and larger size of F-SCs compared to fully terrestrial taxa. However, the vibrissae of these semi-aquatic mammals still do not possess the sensitivity, size, or morphology that is observed in pinnipeds and sea otters (Dehnhardt et al. 1999, Hyvärinen et al. 2009, Marshall et al. 2014). These animals rely on their vibrissae more than terrestrial mammals and often navigate with their eyes closed when under water (Dehnhardt et al. 1999). In fact, blind seals of Lake Saimaa can forage quite well and thrive, presumably using their vibrissa alone (Hyvärinen et al. 1989). This is an indication that this sense of touch has been adapted far beyond that of semi-aquatic and terrestrial mammals.

Not all marine mammals have large, highly innervated vibrissae. The number and use of vibrissae in cetaceans vary greatly. Most odontocetes (toothed whales) lose their vibrissae after birth, while in the Guiana river dolphin (*Sotalia guianesnsis*), which has vibrissal crypts resembling ampullae instead of F-SCs, use them for electroreception (Czech-Damal et al. 2012). Bowhead whales, *Balaena mysticetus,* a mysticete, have approximately 300 vibrissae around their jaw as well as around their blow hole (Drake et al. 2015), presumably for detecting the surface of the water and patches of plankton that they feed upon. Sirenians differ greatly among all marine mammals since all body are vibrissae (Reep et al. 1998, 2002). Florida manatees, *Trichechus manatus latirostris,*

have a wide range of innervation investment depending on the location of the vibrissae (72-225 axons/F-SC) (Reep et al. 2001). Despite the lack of a high innervation per F-SC, their sensitivity to their environment is acute and total innervation investment is high since all hairs are F-SCs and therefore more highly innervated than pelage hairs. The largest F-SCs of all sirenians are associated with their muscular snout and perioral bristles. These modified vibrissae are actively gathering aquatic vegetation and thus are used for both motoric and sensory functions (Marshall et al. 1998). In conclusion, the wide variety in number, size, position, and innervation of vibrissae also demonstrate a wide variety of feeding strategies (e.g. lunge feeding, benthic feeding, hydrodynamic trail following) seen in marine mammals.

5. CONCLUSIONS

The first hypothesis that the largest F-SCs in CSL fit the same innervation pattern as phocids is supported by the data. All pinnipeds studied so far have a similar mean innervation for the largest F-SCs. The second hypothesis that the innervation and microstructure medial to lateral would follow the same pattern that was seen in harp seals (Mattson and Marshall 2016) was not supported according by the data since there were multiple differences between medial to lateral F-SCs, as well as comparing them to similar vibrissal fields in harp seals. This makes sense since CSLs are excel at the active touch behavior, which requires the use of the most medial micro-vibrissae. The third hypothesis that the innervation would increase from dorsal to ventral was supported by the data in that the dorsal to ventral F-SCs showed a similar pattern as the medial to lateral F-SCs. The size and innervation of the F-SCs did increase from dorsal to ventral.

To date, this is the first study to investigate all major areas of the mystacial vibrissal array pinnipeds. CSLs exhibited a decrease in size of UCS in medial and dorsal F-SCs. We saw a general increase of innervation investment from medial to lateral and dorsal to ventral. Ventro-medial and central dorsal F-SCs were very similar in size, morphometrics and innervation. CLSs displayed an asymmetrical distribution of axon bundles in all F-SCs, which has not been reported in phocids. Vascularization was observed in the UCS and blood vessels were seen penetrating the DC in the LCS, which also has not been noted before. The ventral-medial vibrissae possessed the highest

density and the ventral lateral had the lowest density, which differs from harp seals (Mattson and Marshall 2016).

It appears that CSLs do not fit the phocid morphological and innervation pattern but may represent a separate pattern for otariids; additional research needs to be conducted to confirm this new pattern. However, the morphological and innervation pattern (higher axon density in medial F-SCs) is congruent with the behavioral performance work conducted with CSLs, since they are more proficient at active touch compared to hydrodynamic trail following (lateral F-SCs) (Dehnhardt et al. 1994, Dehnhardt et al. 1996, Glaser et al. 2011).

Future directions should include a more detailed investigation of mechanoreceptor and fiber diversity using immunohistochemistry to determine if differences in macro- vs microvibrissae can be distinguished at this neuroanatomical level. I suggest that the next otariid to study should be the Steller sea lion *Eumetopias jubatus,* which has some feeding behavior described which could help add to microstructure and innervation data. Additionally, future areas of study should include investigations of other areas of the mystacial vibrissal fields in phocids where only the lateral most F-SCs have been observed.

REFERENCES

Antonelis, G.A., and Fiscus, C.H., 1980. The pinnipeds of the California Current. CalCOFI Report 21:68-78.

Brecht, M., Preilowski, B., and Merzenich, M.M., 1997. Functional architecture of the mystacial vibrissae. Behavioural Brain Research 84(1):81-97.

Catania, K.C., and Remple, F.E., 2004. Tactile foveation in the star-nosed mole. Brain, Behavior and Evolution 63(1):1-12.

Chernova, O.F., 2006. Evolutionary aspects of hair polymorphism. Biology Bulletin 33(1):43-52.

Czech-Damal, N.U., Liebschner, A., Miersch, L., Klauer, G., Hanke, F.D., Marshall, C., Dehnhardt, G., and Hanke, W., 2012. Electroreception in the Guiana dolphin (*Sotalia guianensis*). Proceedings of the Royal Society of London B: Biological Sciences 279(1729):663-668.

Dehnhardt, G., 1994. Tactile size discrimination by a California sea lion (*Zalophus californianus*) using its mystacial vibrissae. Journal of Comparative Physiology A 175(6):791-800.

Dehnhardt, G., and Kaminski, A., 1995. Sensitivity of the mystacial vibrissae of harbour seals (*Phoca vitulina*) for size differences of actively touched objects. Journal of Experimental Biology 198(11):2317-2323.

Dehnhardt, G., and Dücker, G., 1996. Tactual discrimination of size and shape by a California sea lion (*Zalophus californianus*). Animal Learning & Behavior 24(4):366-374.

Dehnhardt, G., Mauck, B., and Bleckmann, H., 1998. Seal whiskers detect water movements. Nature 394:235-236.

Dehnhardt, G., Hyvärinen, H., Palviainen, A., and Klauer, G., 1999. Structure and innervation of the vibrissal follicle-sinus complex in the Australian water rat, *Hydromys chrysogaster*. Journal of Comparative Neurology 411(4):550-562.

Dehnhardt, G., Mauck, B., Hanke, W., and Bleckmann, H., 2001. Hydrodynamic trail-following in harbor seals *(Phoca vitulina).* Science 293(5527):102-104.

DeLong, R.L., and Stewart, B.S., 1991. Diving patterns of northern elephant seal bulls. Marine Mammal Science 7(4):369-384.

Drake, S.E., Crish, S.D., George, J.C., Stimmelmayr, R., and Thewissen, J.G.M., 2015. Sensory hairs in the bowhead whale, Balaena mysticetus (Cetacea, Mammalia). The Anatomical Record 298(7):1327-1335.

Fay, F.H., 1982. Ecology and biology of the Pacific walrus, *Odobenus rosmarus divergens Illiger*. North American Fauna 1-279

Feldkamp, S.D., DeLong, R.L., and Antonelis, G.A., 1989. Diving patterns of California sea lions, *Zalophus californianus*. Canadian Journal of Zoology 67(4):872-883.

Garcia-Rodriguez, F.J., and Aurioles-Gamboa, D., 2004. Spatial and temporal variation in the diet of the California sea lion (*Zalophus californianus*) in the Gulf of California, Mexico. Fishery Bulletin 102(1):47-62.

George, I.A., and Holliday, C.M., 2013. Trigeminal Nerve Morphology in *Alligator mississippiensis* and Its Significance of Crocodyliform Facial Sensation and Evolution. The Anatomical Record 296:670-680.

Ginter, C.C., Fish, F.E., and Marshall, C.D., 2010. Morphological analysis of the bumpy profile of phocid vibrissae. Marine Mammal Science 26(3):733-743.

Gjertz, I., Kovacs, K.M., Lydersen, C. and Wiig, Ø., 2000. Movements and diving of bearded seal (*Erignathus barbatus*) mothers and pups during lactation and post-weaning. Polar Biology 23(8):559-566.

Glaser, N., Wieskotten, S., Otter, C., Dehnhardt, G., and Hanke, W., 2011. Hydrodynamic trial following in California sea lion (*Zalophus Californianus*). Journal of Comparative Physiology 197:141-151.

Grant, R.A., Haidarliu, S., Kennerley, N.J. and Prescott, T.J., 2013. The evolution of active vibrissal sensing in mammals: evidence from vibrissal musculature and function in the marsupial opossum *Monodelphis domestica*. Journal of Experimental Biology 216(18):3483-3494.

Hanke, W., Wieskotten, S., and Marshall, C., 2013. Hydrodynamic perception in true seals (Phocidae) and eared seals (Otariidae). Journal of Comparative Physiology A 199:421-440.

Hothorn, T., Bretz, F., and Westfall, P., 2008. Simultaneous inference in general parametric models. Biometrical journal 50(3):346-363.

Hyvärinen, H., 1989. Diving in darkness: whiskers as sense organs of the ringed seal (*Phoca hispida saimensis*). Journal of Zoology 218(4):663-678.

Hyvärinen, H., Palviainen, A., Strandberg, U. and Holopainen, I.J., 2009. Aquatic environment and differentiation of vibrissae: comparison of sinus hair systems of ringed seal, otter and pole cat. Brain, Behavior, and Evolution 74(4):268-279.

Jones, A. 2017. Do innervation patterns of mystacial vibrissae in harbor seals, *phoca vitulina*, explain specialization in trail following behavior? Undergraduate thesis, Texas A&M at Galveston, Galveston, TX 1-29.

Kastelein, R.A., and van Gaalen, M.A., 1988. The sensitivity of the vibrissae of a Pacific walrus (*Odobenus rosmarus divergens*) Part 1. Aquatic Mammals 14.3:123-133

King, J.E., 1991. Seals of the world. Comstock Pub. Associates.

Ling, J.K., 1977. Vibrissae of marine mammals. Functional Anatomy of Marine Mammals 3:387-415.

Marshall, C.D., Huth, G.D., Edmonds, V.M., Halin, D.L. and Reep, R.L., 1998. Prehensile use of perioral bristles during feeding and associated behaviors of the Florida manatee (*Trichechus manatus latirostris*). Marine Mammal Science 14(2):274-289.

Marshall, C.D., Kubilis, P.S., Huth, G.D., Edmonds, V.M., Halin, D.L. and Reep, R.L., 2000. Food-handling ability and feeding-cycle length of manatees feeding on several species of aquatic plants. Journal of Mammalogy 81(3):649-658.

Marshall, C.D., Maeda, H., Iwata, M., Furuta, M., Asano, S., Rosas, F. and Reep, R.L., 2003. Orofacial morphology and feeding behaviour of the dugong, Amazonian, West African and Antillean manatees (Mammalia: Sirenia): functional

morphology of the muscular-vibrissal complex. Journal of Zoology 259(3):245-260.

Marshall, C.D., Amin, H., Kovacs, K.M. and Lydersen, C., 2006. Microstructure and innervation of the mystacial vibrissal follicle-sinus complex in bearded seals, *Erignathus barbatus* (Pinnipedia: Phocidae). The Anatomical Record Part A: Discoveries in Molecular, Cellular, and Evolutionary Biology 288(1):13-25.

Marshall, C.D., Rozas, K., Kot, B. and Gill, V.A., 2014. Innervation patterns of sea otter (*Enhydra lutris*) mystacial follicle-sinus complexes. Frontiers in Neuroanatomy 8

Marshall, C.D., Rosen, D.A. and Trites, A.W., 2015. Feeding kinematics and performance of basal otariid pinnipeds, Steller sea lions and northern fur seals: implications for the evolution of mammalian feeding. Journal of Experimental Biology 218(20):3229-3240.

Mattson, E.E. and Marshall, C.D., 2016. Follicle Microstructure and Innervation vary between Pinniped Micro-and Macrovibrissae. Brain, Behavior, and Evolution 88(1):43-58.

Mauck, B., Eysel, U. and Dehnhardt, G., 2000. Selective heating of vibrissal follicles in seals (*Phoca vitulina*) and dolphins (*Sotalia fluviatilis guianensis*). Journal of Experimental Biology 203(14):2125-2131.

McGovern, K.A., Marshall, C.D. and Davis, R.W., 2015. Are Vibrissae Viable Sensory Structures for Prey Capture in Northern Elephant seals, *Mirounga angustirostris?* The Anatomical Record 298:750-760.

Reep, R.L., Marshall, C.D., Stoll, M.L. and Whitaker, D.M., 1998. Distribution and innervation of facial bristles and hairs in the Florida manatee (*Trichechus manatus latirostris*). Marine Mammal Science 14(2):257-273.

Reep, R.L., Marshall, C.D. and Stoll, M.L., 2002. Tactile hairs on the postcranial body in Florida manatees: A mammalian lateral line?. Brain, Behavior and Evolution 59(3):141-154.

Rice, F.L., Mance, A., and Munger, B.L., 1986. A Comparative Light Microscopic Analysis of the Sensory Innervation of the Mystacial Pad. I. Innervation of the Vibrissal Follicle-Sinus Complexes. The Journal of Comparative Neurology 252:154-174.

Sarko, D.K., Reep, R.L., Mazurkiewicz, J.E. and Rice, F.L., 2007. Adaptations in the structure and innervation of follicle-sinus complexes to an aquatic environment as seen in the Florida manatee (Tri*chechus manatus latirostris*). Journal of Comparative Neurology 504(3):217-237.

Stephens, R.J., Beebe, I.J., and Poulter, T.C., 1973. Innervation of the Vibrissae of the California Sea Lion, *Zalophus californianus.* The Anatomical Record 176:421-442.

Wineski, L., 1985. Facial Morphology and Vibrissal Movement in the Golden Hamster. Journal of Morphology 183:199-217.